JOURNAL OF NATURAL PRODUCTS

Article

Cite This: J. Nat. Prod. 2019, 82, 35−44

pubs.acs.org/jnp

Antibacterial Aromatic Polyketides Incorporating the Unusual Amino Acid Enduracididine

Paolo Monciardini,*[,†,‡,∥] Alice Bernasconi,[†,∥] Marianna Iorio,[†] Cristina Brunati,[‡] Margherita Sosio,[†,‡] Laura Campochiaro,[†] Paolo Landini,[§] Sonia I. Maffioli,[†,‡] and Stefano Donadio[†,‡]

[†]NAICONS Srl, Viale Ortles 22/4, 20139 Milano, Italy

[‡]KtedoGen Srl, Viale Ortles 22/4, 20139 Milano, Italy

[§]Bioscience Department, Università degli Studi di Milano, Via Celoria 2, 20122 Milano, Italy

Supporting Information

ABSTRACT: The increasing incidence of infections caused by drug-resistant pathogens requires new efforts for the discovery of novel antibiotics. By screening microbial extracts in an assay aimed at identifying compounds interfering with cell wall biosynthesis, based on differential activity against a *Staphylococcus aureus* strain and its isogenic L-form, the potent enduracyclinones (**1**, **2**), containing the uncommon amino acid enduracididine linked to a six-ring aromatic skeleton, were discovered from different *Nonomuraea* strains. The structures of **1** and **2** were established through a combination of derivatizations, oxidative cleavages, and NMR analyses of natural and $^{13}C-^{15}N$-labeled compounds. Analysis of the biosynthetic cluster provides the combination of genes for the synthesis of enduracididine and type II polyketide synthases. Enduracyclinones are active against Gram-positive pathogens (especially *Staphylococcus* spp.), including multi-drug-resistant strains, with minimal inhibitory concentrations in the range of 0.0005 to 4 $\mu g\ mL^{-1}$ and with limited toxicity toward eukaryotic cells. The combined results from assays and macromolecular syntheses suggest a possible dual mechanism of action in which both peptidoglycan and DNA syntheses are inhibited by these molecules.

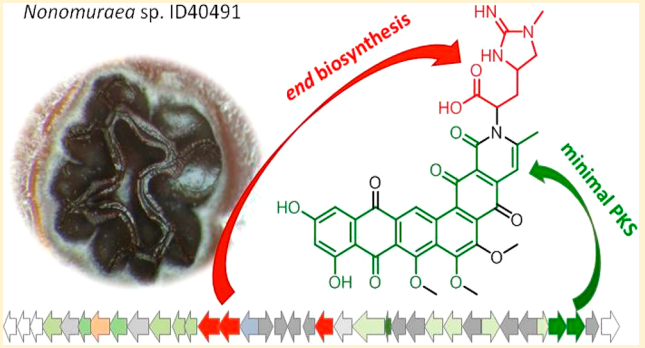

Our ability in controlling infections, which has been taken for granted for decades after the introduction in clinical practice of antibiotics, is currently at risk due to the continuous rise of infections sustained by antibiotic-resistant microorganisms. Multi-drug-resistant pathogens are now routinely isolated, severely impairing our ability to manage bacterial infections.[1,2] To address this threat to human (and animal) health requires increased efforts toward discovery and development of novel anti-infective substances, not affected by prevailing resistance mechanisms.[1,2] Ideally, novel antimicrobials should belong to new chemical classes to minimize cross-resistance with marketed antibiotics.[3] Natural products represent a major source of approved antibacterials:[4,5] the majority of antibiotics in clinical use are microbial metabolites or their derivatives, typically from actinomycetes.[2,4] Despite extensive screening during the "golden era" of antibiotic discovery, molecules with novel structures and modes of action can still be found among microbial metabolites. Recent examples include teixobactin[6] and pseudouridimycin,[7] which, although acting on well-established bacterial targets (cell wall and RNA biosynthesis, respectively), do so with mechanisms differing from those of other molecules targeting the same pathways and thus are active against resistant pathogens.

In our search for novel classes of antibacterial molecules, we have previously described an approach based on mining our proprietary database, which contains results of several antibacterial high-throughput-screening (HTS) assays performed on more than 100 000 microbial extracts.[8] While HTS applies rigid filters for identifying a workable number of candidates for further analyses, *a posteriori* evaluation of the HTS data permits selection of candidates that were not previously pursued. By re-evaluating data from an HTS phenotypic screen aimed at identifying molecules inhibiting bacterial cell wall biosynthesis,[9] we have reported different lanthipeptides,[10,11] including compounds with unusual structural features and unexpected bioactivities.[10−12]

Here we further expand on this data mining approach and report on the isolation of aromatic polyketides containing the uncommon amino acid enduracididine installed on a fused six-ring skeleton. These molecules, dubbed enduracyclinones, are highly active against Gram-positive pathogens, including antibiotic-resistant strains.

Received: May 4, 2018
Published: January 7, 2019

DOI: 10.1021/acs.jnatprod.8b00354
J. Nat. Prod. 2019, 82, 35−44

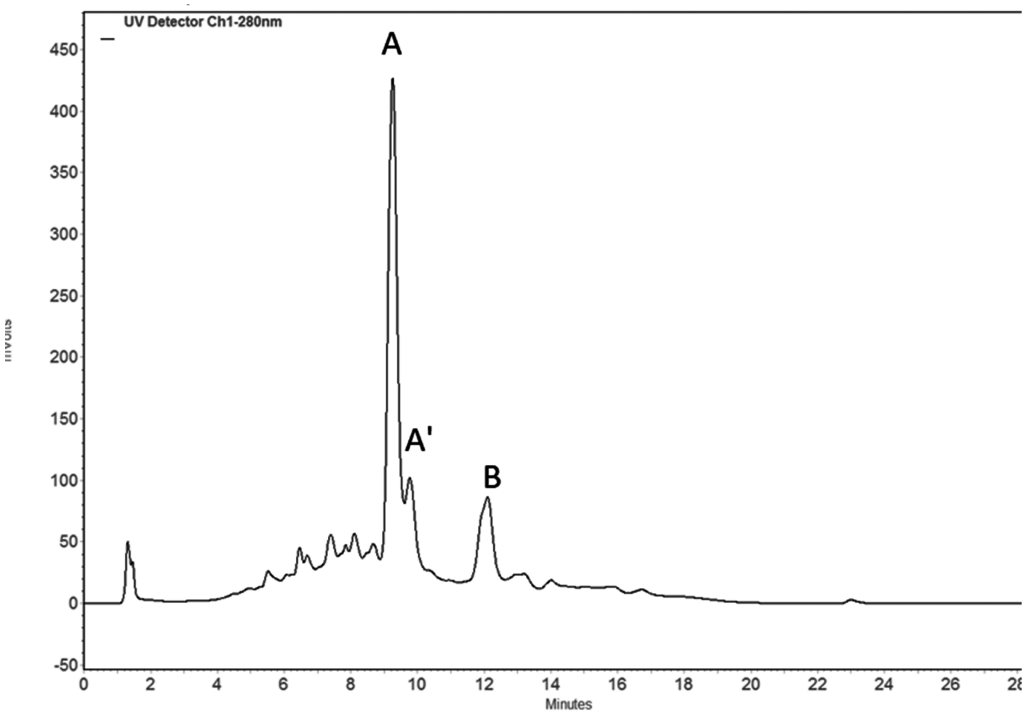

Figure 1. HPLC trace of an ethanol extract from strain ID40491 (see text for details).

RESULTS AND DISCUSSION

Data Mining. The HTS database contains data on a phenotypic assay aimed at identifying likely inhibitors of bacterial cell wall biosynthesis. About 120 000 microbial fermentation extracts were analyzed by an assay based on differential activity against a *Staphylococcus aureus* strain and its isogenic L-form, i.e., a variant empirically adapted to grow in the absence of a cell wall in an osmotic-protective medium.[9] Extracts inhibiting growth of *S. aureus* at a concentration at least 8 times lower than that required for growth inhibition of the L-form were assumed to interfere with cell wall biosynthesis. Positive samples were further assayed for maintenance of activity after incubating the extracts with beta-lactamases or with D-Ala-D-Ala (these tests were meant to discard β-lactamase-sensitive compounds and D-Ala-D-Ala binders, respectively) before further characterization. By searching the HTS database, however, we identified 17 extracts that, albeit fulfilling the selection criteria (lack of or reduced activity against L-forms), had not been further analyzed during the original screening. The corresponding strains were therefore processed, and the extracts obtained from 12 cultures confirmed activity against *S. aureus*. Ten of these extracts retained activity against one multi-drug-resistant (MDR) *S. aureus* strain and were further processed (Supplementary Table S1). One extract was found to contain the lantibiotic NAI-802,[10] a variant of actagardine likely to target cell wall biosynthesis, and another extract was found to contain the thiopeptide nosiheptide, a molecule whose primary target is translation but which, for unknown reasons, is known to be less active against L-forms.[13] The other eight strains produced the same compound, as described below.

Discovery of Enduracyclinones from *Nonomuraea* spp. Extracts from the eight strains contained the same active fractions correlating to peaks with retention times of 9.5 (major peak), 10, and 12 min (peaks A, A′, and B, respectively, as shown in Figure 1). The peaks showed m/z $[M + H]^+$ of 711, 697, and 713, respectively, and similar UV−vis spectra (absorption maxima were at 244, 283, 334, and 445 nm for peak A). The molecules appeared to be very stable in MS fragmentation conditions, with the ready loss of only a 44 amu fragment.

The corresponding eight actinomycete strains were analyzed by comparing their nearly complete 16S rRNA gene sequences and assigned to three distinct lineages within the genus *Nonomuraea* (Supplementary Table S1). One of the lineages is represented by six strains isolated from four soil samples collected in different locations in Italy or from plant specimens from Scotland and Italy. These strains showed 99.7−100% identity in the 16S rRNA gene sequences among themselves and to *Nonomuraea endophytica*. The two additional lineages are represented by a single strain each, originating from Kenyan and Honduras soils and showing relatively low 16S identity with described species (98.4% with *Nonomuraea candida* or 98.9% with *Nonomuraea salmonea*). Comparable levels of the peaks correlated to biological activity were observed for the six European strains, and strain ID40491 was chosen for further analyses. Under the best conditions, strain ID40491 produced about 500 mg L^{-1} peak A. The remaining European strains produced at least 100 mg L^{-1} peak A.

Purification and Structure Elucidation. The active peaks were associated with both the mycelium and the cleared broth. Therefore, both mycelium and cleared broth were processed, and the active compounds were retrieved by exploiting their low aqueous solubility at pH 5 and their increased solubility at pH 9. Further purification afforded a sample containing HPLC peaks A and A′ in a 9:1 ratio and another containing A, B, and A′ in a 5:3:2 ratio. From the first sample a small amount of a highly pure A peak sample was generated (see Experimental Section for purification procedures). To help structure elucidation, the $^{13}C-^{15}N$-labeled compounds were also prepared by growing strain ID40491 in a uniformly labeled medium (see Experimental Section) that

DOI: 10.1021/acs.jnatprod.8b00354
J. Nat. Prod. 2019, 82, 35−44

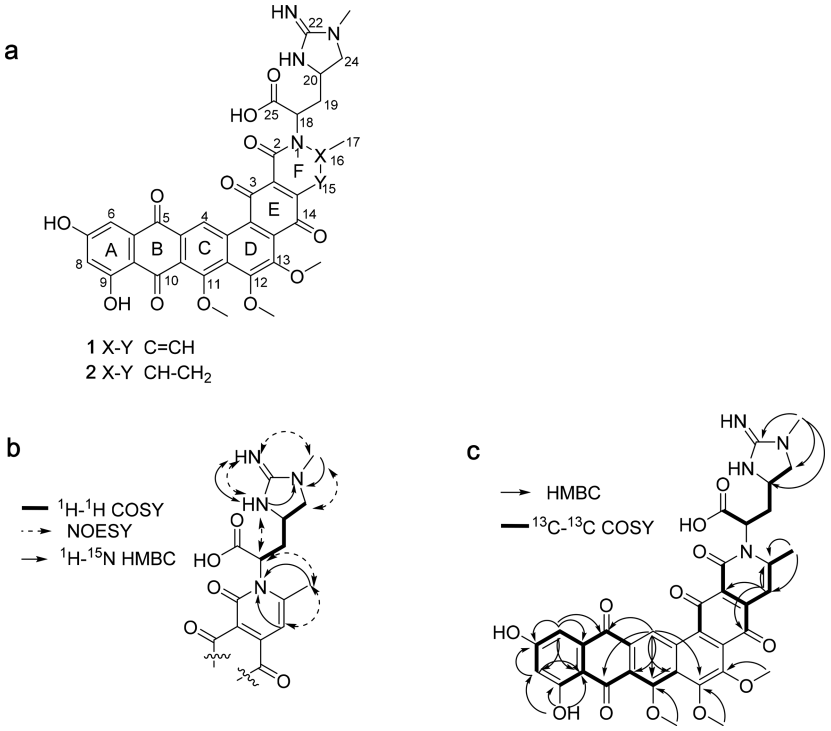

Figure 2. Structures of compounds and NMR correlations. (a) Structures of **1** and **2**. (b) Main ^{1}H−^{1}H COSY, NOESY, and ^{1}H−^{15}N HMBC correlations. (c) Observed HMBC and ^{13}C−^{13}C COSY correlations of **1**.

afforded a purified sample of peaks A and A′ (in a 9:1 ratio) with a 95% ^{13}C- and ^{15}N-enrichment (Supplementary Figure S1). Unless otherwise stated, all chemical and bioactivity analyses were performed on samples containing peaks A and A′ in a 9:1 ratio.

The main congener **1** (peak A) has a molecular formula of $C_{36}H_{30}N_4O_{12}$ with 24 double-bond equivalents, as deduced by high resolution mass spectrometry (HRMS). In the presence of trimethylsilyldiazomethane, a 14 amu heavier product was formed, consistent with a methyl ester of **1**, while *N*,*N*-dimethylpropylamine in the presence of condensing agents converted **1** into a *m*/*z* 795 $[M + H]^+$ compound, consistent with the formation of the corresponding amide. The MS/MS data (loss of 44 amu, see above) and the results from these reactions suggested the presence of a free carboxylic acid. The structure of **1** (Figure 2) was established by a combination of one- and two-dimensional NMR analyses, performed on the natural and the ^{13}C−^{15}N-labeled compound, and confirmed by selective oxidative cleavage, as explained below.

1D and 2D NMR analyses established the presence of a polycyclic aromatic system linked to a nitrogen-rich aliphatic acid. The ^{1}H NMR data (Table 1, Figure 2) of **1** displayed four aromatic protons at δ_H 9.58, 6.80, 7.14, and 6.64 ppm, the latter two showing a meta-coupling constant (J = 2.1 Hz); three methoxy (δ_H 3.98, overlapped), one *N*-methyl (δ_H 2.89) and one C-methyl (δ_H 2.59); two nitrogen-bound protons at δ_H 8.17 and 8.03 ppm; and two phenolic signals at δ_H 11.30 and 13.30 ppm. In addition, the major spin system corresponded to a four-carbon chain formed by an amino acid-alpha proton at δ_H 5.05 ppm (H-18) directly connected to a CH_2 at 2.02−2.73 ppm (H-19a and b), followed by another CH at 4.09 ppm (H-20) and a further diasterotopic methylene at 3.30−3.84 ppm (H-24a and b). The analysis of proton and carbon chemical shifts (Table 1) together with correlation spectroscopy (COSY), total correlation spectroscopy (TOCSY), and nuclear Overhauser enhancement spectroscopy (NOESY) correlations suggested that C-20 and C-24 are trapped in a rigid structure. Furthermore, a guanidine unit was identified through the heteronuclear multiple bond correlation (HMBC) of the *N*-methyl group to an sp^2 carbon at δ_C 158.2 ppm (C-22) and the NOESY signals of the proton at 8.02 ppm with the proton at 8.17 ppm and the *N*-methyl group. Moreover, the NOESY correlation of the *N*-methyl group with one of the methylene protons at C-24 (H-24b, at δ_H 3.84 ppm) and of the alpha proton at 5.05 ppm with the proton at 8.17 ppm and with the C-methyl at 2.59 ppm established that the rigid structure is a five-membered ring arising from an *N*-methyl enduracididine linked through the α-amino group to the aromatic system.

Heteronuclear single quantum coherence (HSQC), HMBC, and monodimensional ^{13}C experiments highlighted the presence of four quinonic carbonyls at δ_C 181.4, 181.9, 182.4, and 185.6 ppm, a carboxyl carbon at δ_C 169.8, and two other carbonyls at δ_C 158.0 and 158.2. A key signal was the aromatic CH-4, with a peculiar chemical shift at δ_H 9.58 ppm, correlating to a carbon at δ_C 125 ppm. It is known that aromatic hydrogens *peri* to quinones in natural anthraquinones are deshielded, with values ranging from 7.5 to 8.3 ppm.[14,15] In our case, H-4 appeared even more deshielded, suggesting the presence of a second quinone (E ring), linked angularly to the tetracyclinone (A−D rings). Moreover, this proton gave HMBC correlations with quinones C-5 and C-10, aromatic carbons C-10a and 11a, and the methoxy-substituted aromatic carbons C-11 and C-12, thus establishing the core A−E ring structure.

The relative position of the two quinone moieties was confirmed by treatment with 20% H_2O_2 at 60 °C (see Experimental Section for details).[16,17] Under these conditions both quinones were oxidatively cleaved, leading to the formation of a major species at *m*/*z* 637 $[M + H]^+$,

DOI: 10.1021/acs.jnatprod.8b00354
J. Nat. Prod. 2019, 82, 35−44

Table 1. NMR Spectroscopic Data (300 MHz, DMSO-d_6) for Enduracyclinone A in DMSO-d_6

position	δ_C, type	δ_H (J in Hz)	δ_N, type
1			197.3, N
2	158.0, C		
2a	118.7, C		
3	182.3, C		
3a	129,8, C		
3b	131.2, C		
4	125.5, CH	9.58, s	
4 a	130.6, C		
5	181.4, C		
5a	134.8, C		
6	107.3, CH	7.14, d (2.1)	
7	164.8, C		
OH(7)		11.30, br s	
8	108.4, C	6.64, d (2.1)	
9	165.1, C		
OH(9)		13.30, s	
9 a	111.6, C		
10	185.6, C		
10a	122.1, C		
11	159.2, C		
OMe (11)	63.2, CH_3	3.98 s	
11a	130.5, C		
12	155.6, C		
OMe (12)	62.6, CH_3	3.98 s	
13	150.8, C		
OMe (13)	61.9, CH_3	3.97 s	
13a	130.4, C		
14	181.9, C		
14a	143.6, C		
15	101.8, CH	6.80 s	
16	155.5, C		
17	22.3, CH_3	2.59, s	
18	56.6, CH	5.05, m	
19	35.1, CH_2	2.02, m−2.73, m	
20	50.9, CH	4.09, m	
21 NH		8.17, br s	90.4, NH
22	158.2, C		
22 NH		8.02 br s	71.3, NH
23			77.0, N
Me (23)	31.4, CH_3	2.89, m	
24	55.2, CH_2	3.38, m−3.84, m	
25	169.8, C		

corresponding to the dicarboxylic product **ox-1** following rupture of ring B (Figure 3), and of species at m/z 469 $[M + H]^+$ (product **ox-2**) and m/z 279 $[M + H]^+$ (product **ox-3**), after breaking ring E.

HMBCs of the two aromatic protons with meta-coupling constant (J = 2.1 Hz) enabled placing the substituents on ring A, with positions 7 and 9 bearing two phenols with different NMR behavior: while OH-7 gives a broad singlet with no significant 2D correlations, OH-9 presents a sharp signal at δ_H 13.30 ppm with HMBC correlations to C-8, C-9, and C-9a, suggesting that the phenol partakes in an intramolecular hydrogen bond with the quinone oxygen in *peri* position. The last ring, F, was established as a benzofused methyl-pyrimidone ring thanks to the HMBC correlations of proton H-15 at δ_H 6.80 ppm with quinone C-14, carbons C-2a and C-16, and methyl 17.

$^1H-^{15}N$-HMBC and $^{13}C-^{13}C$ COSY analyses of $^{13}C-^{15}N$-labeled **1** allowed the assignment of all nitrogen chemical shifts and the identification of the cyclic amide, with N-1 correlating to CH_3-17 and CH-15 (Table 1). Moreover, the majority of the carbon backbone connectivity of **1** was clearly established (Figure 2C).

As shown above (Figure 1), strain ID40491 produced also two minor congeners. Peak A′ showed a difference of 14 amu in comparison to **1**, suggesting the lack of a methyl group (found m/z 697.1786 $[M + H]^+$ for $C_{35}H_{28}N_4O_{12}$, calcd 697.1776). During oxidative cleavage, we also observed the formation of a minor m/z 455 $[M + H]^+$ species along with product **ox-2** (Figure 3), consistent with the lack of one of the three methoxy groups in rings C or D. However, the amount of des-methyl-**1** was insufficient for further analyses, so the exact position of the free OH in this minor congener remains to be established.

HRMS indicated that peak B was associated with a $C_{36}H_{32}N_4O_{12}$ species (compound **2** in Figure 2) with 23 unsaturations (found m/z 713.2104 $[M + H]^+$, 713.2095 calcd). The observation that, in the ^1H NMR spectrum of **1**:**2**:desmethyl-**1** 5:3:2, Me-17 integrated less than expected and that **2** easily converted into **1** under oxidative conditions (see Experimental Section) suggested that **2** differs from **1** for the lack of the unsaturation in the pyrimidone ring F (Figure 2).

Structural Features of Enduracyclinones. Overall, the metabolites produced by strain ID40491 consist of a highly oxygenated angular hexacyclic framework linked to an *N*-methylated enduracididine moiety. We therefore named the compounds enduracyclinones A (**1**) and B (**2**).

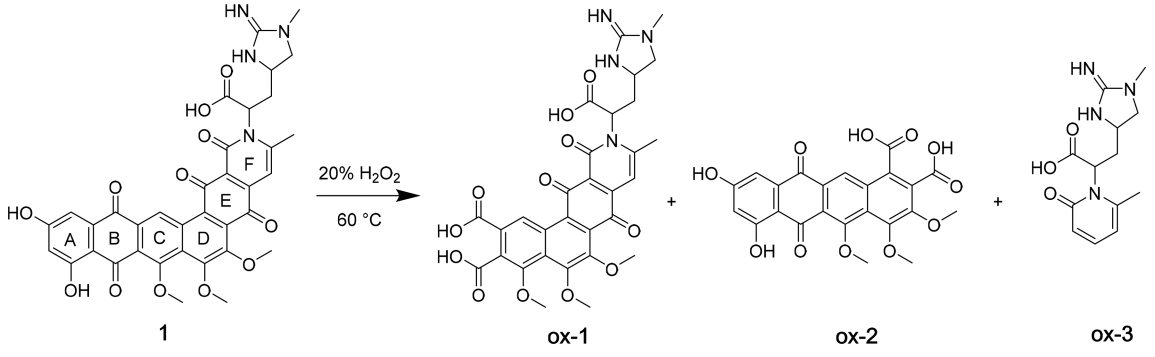

Figure 3. Oxidative cleavage of **1**.

DOI: 10.1021/acs.jnatprod.8b00354
J. Nat. Prod. 2019, 82, 35−44

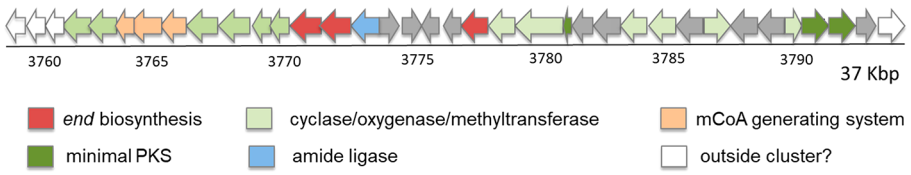

Figure 4. Organization of the enduracyclinone biosynthetic genes. The deduced functions are color-coded as indicated and summarized in Table 2. *end*, enduracididine; mCoA, malonyl-CoA.

Table 2. Coding DNA Sequences (CDSs) from the *edc* Cluster of *Nonomuraea* sp. ID40491 and Proposed Roles in the Pathway

edc CDS	size (aa)	homologue (strain, accession no.)[a]	identity (%)	putative role
Chr_03759	115	Transposase (*Nonomuraea coxensis*, WP_026213651)	85	outside cluster
Chr_03760	612	hypothetical protein (*Streptomyces* sp., CNS335)	68	unknown, outside cluster?
Chr_03761	219	DNA repair protein (*Nonomuraea* sp. NBRC 110462, WP_055503593.1)	77	unknown, outside cluster?
Chr_03762	350	*O*-methyltransferase (*Micromonospora echinospora*, ADB23385)	45	cyclase-methyltransferase
Chr_03763	219	putative leucyldemethylblasticidin S guanidine methyltransferase (*Streptomyces griseochromogenes*, AAP03126.1)	51	methyltransferase
Chr_03764	448	PdmP1, biotin carboxylase (*Actinomadura hibisca*, ABM21735.1)	61	subunit of acetyl carboxylase
Chr_03765	156	biotin carboxyl carrier protein of acetyl-CoA carboxylase (*Streptomyces lydicus*, AJT61720.1)	47	subunit of acetyl carboxylase
Chr_03766	542	acetyl carboxylase (*Streptomyces* sp. R1128, AAG30193.1)	60	subunit of acetyl carboxylase
Chr_03767	191	GrhU, monooxygenase (*Streptomyces* sp. JP95, AAM33683.1)	53	monooxygenase
Chr_03768	154	putative monooxygenase (*Streptomyces flavogriseus*, ADE22312.1)	39	monooxygenase
Chr_03769	150	RubF, putative polyketide cyclase/reductase (*Streptomyces collinus*, AAG03070.2)	67	cyclase/reductase
Chr_03770	107	putative cyclase (*Streptomyces collinus*, AAG03065.2)	71	cyclase
Chr_03771	372	PLP-dependent aminotransferase MppQ (*Streptomyces hygroscopicus*, AAU34210)	54	enduracididine biosynthesis
Chr_03772	374	enduracididine biosynthesis enzyme MppP (*Streptomyces hygroscopicus*, AAU34209)	63	enduracididine biosynthesis
Chr_03773	613	PdmN, asparagine synthetase (*Actinomadura hibisca*, ABK58686.1)	50	enduracididine-polyketide amide synthase
Chr_03774	249	ABC transporter (*Micromonospora* sp., ALA09377.1)	58	export
Chr_03775	649	Sio5, ABC transporter (*Streptomyces sioyaensis*, ACN80636.1)	30	transporter
Chr_03776	217	Azi47, DNA-binding response regulator (*Streptomyces sahachiroi*, ABY83185.1)	63	DNA-binding response regulator
Chr_03777	445	regulatory protein D (*Actinoplanes friuliensis*, CAM56777.1)	44	regulator
Chr_03778	270	conserved hypothetical protein MppR (*Streptomyces hygroscopicus*, AAU34211.1)	65	enduracididine biosynthesis
Chr_03779	317	EpaU, cytochrome oxidase subunit II (*Kitasatospora* sp. HKI 714, AHW81480.1)	39	oxidase
Chr_03780	419	EpaT, cytochrome ubiquinol oxidase (*Kitasatospora* sp. HKI 714, AHW81479.1)	56	oxidase
Chr_03781	85	ACP (*Streptomyces griseus*, CAE17520.1)	62	ACP
Chr_03782	512	putative efflux protein (*Streptomyces kanamyceticus*, CAF60521.1)	38	transporter
Chr_03783	32	putative protease (*Streptomyces olivoviridis*, BAN83926.1)	47	unknown
Chr_03784	494	FAD-dependent monoxygenase (*Micromonospora echinospora*,ADB23401.1)	48	monoxygenase. hydroxylase
Chr_03785	338	putative O-methyltransferase (*Streptomyces tendae* Tu 4042, CAM34375.1)	49	*O*-methyltransferase
Chr_03786	498	putative peptide transporter (*Streptomyces griseus* ATCC 43944, AAQ08913.1)	50	transporter
Chr_03787	393	cytochrome P450 (*Streptomyces* sp. TA-0256, BAJ52675.1)	53	monoxygenase
Chr_03788	221	LuxR transcriptional regulator (uncultured bacterium, AHX24716.1)	65	regulator
Chr_03789	373	two component system histidine kinase (uncultured bacterium, AHX24717.1)	40	regulator
Chr_03790	137	cyclase (uncultured bacterium, AHX24700.1)	69	polyketide cyclase
Chr_03791	420	polyketide beta-ketoacyl synthase alpha (*Streptomyces flavogriseus*, ADE22315.1)	77	KSα
Chr_03792	400	Hex23, polyketide beta-ketoacyl synthase beta (*Streptosporangium* sp. CGMCC 4.7309, AMK51280.1)	66	KSβ
Chr_03793	259	DacT1, DNA-binding response regulator (*Dactylosporangium* sp. SC14051, AFU65883.1)	49	transcriptional regulator
Chr_03794	514	twin-arginine translocation pathway signal sequence (*Kibdelosporangium aridum*, SMD27155)	64	outside cluster?

[a]Best match observed by BLAST analysis of clusters listed in the MIBIG database of validated biosynthetic gene clusters[37] or from the nonredundant GenBank database. Abbreviations: ACC, acetylCoA carboxylase; ACP, acyl carrier protein; BCCP, biotin carboxylate carrier protein; KSα, type II polyketide synthase β-ketoacyl synthase, alpha subunit; KSβ, type II polyketide synthase β-ketoacyl synthase, beta subunit.

Similar polyketide skeletons are present in echinosporamicin[18] and related molecules[19] and in the polycyclic xanthone antibiotics,[20] but with differences in the saturation degree and decoration of the aromatic rings. Like echinosporamicins, enduracyclinones present a 1,4-benzoquinone moiety (ring B), instead of the gamma-pyrone found in the polycyclic xanthones, and a second quinone (ring E), an uncommon feature of xanthones. Indeed, xantholipin is the only representative of this class with a quinone in ring E, which is usually monooxygenated (as in cervinomycin and actinoplanone) or contains a para-biphenol (i.e., simaomycin and kibdelone).[20] The three adjacent oxygens present in rings C and D of enduracyclinones are found only in some polycyclic xanthones (lysolipin I and FD-594),[20] where ring D is

DOI: 10.1021/acs.jnatprod.8b00354
J. Nat. Prod. 2019, 82, 35−44

nonaromatic, but not in echinosporamicins. Position C-4 is oxygenated in all xanthones[20] and echinosporamicins[19] but unmodified in **1** and **2**, rendering the ABC ring system of enduracyclinones identical to bequinostatin's, which however lacks the ring C methoxy and substantially differs in the remaining portion of the molecule.[21]

Most polycyclic xanthones and echinosporamicins present a cyclic amide (ring F), which can be substituted on the nitrogen with amine, methyl, or amino acid-derived heterocyclic structures. In particular, echinosporamicin carries a Gly-Ala-Ser tripeptide,[18] with the serine condensed on the alanine to form a piperazinone moiety, whereas an oxazolidine ring is fused to the pyrimidone in cervinomycin.[20] The unique feature of enduracyclinones is the presence of an *N*-methyl enduracididine moiety contributing to ring F. Enduracididine is an uncommon amino acid arising from arginine oxidization and cyclization and characterized by a guanidine embedded in a five-membered ring. Enduracididine has been so far encountered in a small number of natural products, where it can also be decorated with a β-hydroxy group.[22] In most cases (enduracidin, mannopeptimycin, and teixobactin), enduracididine incorporation proceeds through a nonribosomal peptide synthase (NRPS) assembly line, whereas in minosaminomycin the enduracididine moiety is linked to an amino sugar through an amide bond and carbamoylated at its α-nitrogen. Thus, enduracyclinones represent the first example of an enduracididine-containing aromatic polyketide and the first report of an *N*-methylated enduracididine moiety and represent another example of actinomycetes' ability in performing combinatorial biosynthesis by joining different pathways for the generation of chemical diversity.

Enduracididine contains two stereogenic carbons that can occur in microbial metabolites in any R/S combination.[22] The stereochemistry of the enduracididine moiety in **1** could not be established experimentally. Indeed, the amide bond linking enduracididine to the polyketide core is trapped in a pseudo-aromatic ring, preventing easy release of this amino acid and direct comparison with suitable standards. The free rotation around the methylene in beta position (C-19) prevents using NMR data for relative stereochemistry assignment. As explained below, the enduracyclinone biosynthetic gene cluster (BGC) contains homologues of genes involved in L-enduracididine (i.e., 2*S*-4*R*-enduracididine) biosynthesis.[23,24] Since the D-enduracididine isomers occurring in enduracidin and mannopeptimycin are reported to be generated by NRPS-catalyzed epimerization at the α-carbon[23,25] and the enduracyclinone BGC does not apparently encode epimerases, it is reasonable to assume that the stereochemistry of the enduracididine moiety in **1** is *S* and *R* for the alpha (C18) and gamma (C20) carbons, respectively.

Putative Enduracyclinone Biosynthetic Gene Cluster. The structure of enduracyclinone suggested that it is generated from a (partially cyclized) tridecaketide intermediate condensed to an (*N*-methyl)-enduracididine, followed by formation of ring F. Oxidation at C-5, C-13, and C-14 and the three *O*- methylations might precede or follow ring F formation. To search for the enduracyclinone BGC, we scanned a draft genome sequence of *Nonomuraea* sp. ID40491, using the antiSMASH platform (https://antismash-secondarymetabolites.org) for the presence of an aromatic polyketide gene cluster associated with genes specifying for L-enduracididine biosynthesis. The likely enduracyclinone (*edc*) cluster encompasses a 37 kbp segment and includes 35 CDSs. By bioinformatic analysis we could assign a putative role to almost all genes in the cluster and establish its likely boundaries, as depicted in Figure 4 and summarized in Table 2.

The biosynthesis of L-enduracididine has been established for the mannopeptimycin pathway; it involves MppP, a PLP-dependent aminotransferase proposed to convert L-Arg into 2-oxo-4-hydroxy-5-guanidinovaleric acid, which is then cyclized by MppR and transaminated by MppQ, using L-Ala as amino donor.[24] Proteins showing 81%, 68%, and 75% identity to MppP, MppQ, and MppR, respectively, are encoded by a three-gene cassette (*endPQR*) in the enduracidine gene cluster.[23] ORFs with 63−62%, 54−56%, and 65−66% identity to *MppP/EndP*, *MppQ/EndQ*, and *MppR/EndR*, respectively, are present in the *edc* cluster, although only the former two genes are adjacent (Figure 4). The *edc* cluster encodes a protein (Chr_03773) with 50% identity to PdmN, an asparagine synthase-like enzyme involved in the biosynthesis of pradimicin, a dodecaketide linked through an amide bond to an Ala residue.[26] Thus, Chr_03773 is the likely amino acid ligase attaching (*N*-methyl)enduracidin to a tridecapolyketide precursor.

Synthesis of the enduracyclinone carbon backbone is expected to require a type II PKS. Accordingly, the *edc* cluster encodes a ketosynthase, chain length factor (CLF), and acyl carrier protein, although the latter gene is not immediately downstream of the CLF-encoding gene (Figure 4 and Table 2). The *edc* cluster encodes also three polyketide cyclases, four monooxygenases, two methyltransferases, two oxidases, and a bifunctional cyclase-methyltransferase. The *edc* cluster also encodes a malonyl-CoA-generating system (the three components of a biotin-dependent carboxylase for generating the malonyl-CoA extender units), recently found also in the paramegnetoquinone gene cluster from *Actinoallomurus*.[27] In addition, the cluster encodes five regulators, four transporters, and three proteins of unknown function (Figure 4 and Table 2). Final confirmation of the role of the described cluster in enduracyclinone biosynthesis should be obtained by genetic manipulation (e.g., by generation of knockout mutants or by heterologous expression), which was beyond the scope of our work. However, it would also be interesting to analyze the genomes of the other seven producers to check whether they contain the identified cluster.

Biological Activity of Enduracyclinones. Enduracyclinone A (**1**) showed good activity against staphylococci and streptococci, with MICs ranges of 0.0005−0.03 and 0.25−0.5 μg mL^{-1}, respectively (Table 3). Activity was also observed against enterococci (MICs 2−4 μg mL^{-1}), *Clostridium difficile* (2 μg mL^{-1}), and *Propionibacterium acnes* (0.25 μg mL^{-1}). No activity was observed against *Mycobacterium smegmatis*, Gram-negative bacteria, or *Candida albicans*. Identical activity against *S. aureus* ATCC 6538P was obtained for purified compound **1** and for the mixture containing **1** and its des-methyl derivative in a 9:1 ratio, ruling out the possibility that the observed biological activity derived only from peak A′. As expected from its structural novelty, enduracyclinone A (**1**) was equally active against one strain each of *S. aureus* and of *Staphylococcus hemolyticus* with multiple resistance to clinically used antibiotics. Time-kill experiments with two different *S. aureus* strains indicated a rapid bactericidal activity, with >99.9% killing within 2 to 4 h at 8× MIC. Longer incubations (i.e., 24 h) led to an increase in viable cell counts, comparable to untreated controls (Supplementary Figure S2).

DOI: 10.1021/acs.jnatprod.8b00354
J. Nat. Prod. 2019, 82, 35−44

Table 3. Antibacterial Activity of Enduracyclinone A (1), Vancomycin (Van), and Gentamicin (Gen) expressed as MIC values

strain[a]	resistance[b]	MIC (μg mL^{-1})		
		1	Van	Gen
Staphylococcus aureus ATCC 6538P		0.004	0.5	0.5
Staphylococcus aureus ATCC 29213		0.0005	1	0.5
Staphylococcus aureus L3864	Met^R	0.03	1	>128
Staphylococcus aureus L3797	Met^R, AGs^R, Cip^R, Cli^R, Van^I	0.03	8	64
Staphylococcus hemolyticus L1730		0.03	2	>128
Staphylococcus hemolyticus L1729	Met^R Tet^R, AGs^R, Cip^R	0.015	2	>128
Staphylococcus intermedius ATCC 29663		0.007	1	≤0.125
Streptococcus pyogenes L49		0.5	0.25	16
Streptococcus pneumoniae ATCC BAA1407	*ermB*, *mefE*	0.25	0.5	64
Streptococcus pneumoniae L44		0.25	0.125	8
Enterococcus faecium L568		4	1	32
Enterococcus faecium L569	VanA	2	>128	16
Propionibacterium acnes ATCC 25746		0.25	0.25	2
Clostridium difficile ATCC 17858		2	0.5	128

[a]Strains designated with an L prefix are clinical isolates (collected in Italy or USA) from the NAICONS collection. Other strains are from the American Type Culture Collection, USA. [b]The superscript R indicates resistance to methicillin (Met), aminoglycosides (AGs), ciprofloxacin (Cip), clindamycin (Cli), or tetracyclin (Tet); the superscript I indicates intermediate resistance to vancomycin (Van); *ermB* and *mefE* indicate the known genetic determinants conferring resistance to macrolides−lincosamides−streptogramins by ribosomal methylation and to macrolides by efflux, respectively. VanA designates vancomycin-inducible resistance to glycopeptides by lipid II modification.

Comparably low MIC values vs Gram-positive bacteria have been reported for some structurally related compounds, such as lysolipin I,[28] cervinomycin,[29] and echinosporamicins.[19] It should be noted that several of these molecules exhibited cytotoxic activity to tumor cell lines at concentrations comparable to or lower than the MIC,[20] e.g., actinoplanone, simaomicin, and xantholipin[30−32] and echinosporamicin-related compounds.[19] When evaluated on the cancer cell line PANC-1 or the non-cancer cell line HEK-293, enduracyclinone A (**1**) showed only 20% inhibition at 90 μM or an IC_{50} of 55 μM, respectively (Supplementary Figure S3). Thus, in comparison with the previously mentioned molecules, enduracyclinone A shows little cytotoxicity against the tested cell lines.

As mentioned above, the enduracyclinone-containing extracts were selected for their ≥8-fold higher activity on WT *S. aureus* than on the corresponding L-form (Supplementary Table S1), indicating that peptidoglycan-devoid cells are less sensitive than the parental cells. When tested against *Bacillus subtilis* BAU102, a reporter strain that detects most classes of cell wall inhibitors,[13] enduracyclinone A (**1**) elicited a signal compatible with cell wall inhibition and distinct from that caused by detergents (Supplementary Table S2). We then evaluated the effect of enduracyclinone A (**1**) on macromolecular synthesis in *S. aureus*, observing a dose-dependent inhibition of DNA and cell wall biosynthesis, with comparable IC_{50} values (2 and 5 μg mL^{-1}, respectively). While RNA synthesis was only marginally affected, incorporation of label into proteins appeared to be stimulated by enduracyclinone A (Supplementary Figure S4).

Overall, the results from the L-form assay, the reporter assay, and macromolecular syntheses are consistent with inhibition of cell wall biosynthesis by enduracyclinone A, although DNA synthesis is also likely to be affected. There are few reports on the mechanism of action of structurally related molecules. Lysolipin has been proposed to target bactoprenol-containing molecules and inhibit cell wall biosynthesis, based on inhibition of peptidoglycan synthesis and concomitant accumulation of lipid-bound precursors in *B. subtilis*.[28] On the basis of its effect on macromolecular syntheses, solute leakage, and reversion assays in *S. aureus*, cervinomycin has been proposed to interfere with membrane functions by interaction with phospholipids.[33] Inhibition of DNA synthesis, interference with cell cycle regulation, or generation of reactive oxygen species was proposed for the cytotoxic effects of different polycyclic xanthones.[30,31,34] Interestingly, while minosaminomycin (structurally similar to the aminoglycoside kasugamycin) interferes with initiation of protein synthesis,[35] the other enduracididine-containing antibiotics (teixobactin, enduracidine, and mannopeptimycin) inhibit cell wall biosynthesis by binding to lipid II.[36] Thus, it is tempting to speculate that appending a positively charged, rigid amino acid on a flat, hydrophobic skeleton might enhance affinity for cell wall intermediates, endowing enduracyclinone A with a dual mechanism of action.

These potent antibacterial compounds, produced at high levels by at least three different *Nonomuraea* lineages, had so far apparently escaped detection. This bodes well for discovering new classes of antibacterial agents from actinomycetes.

EXPERIMENTAL SECTION

General Experimental Procedures. ^{1}H and ^{13}C 1D and 2D NMR spectra (COSY, TOCSY, NOESY, HSQC, HMBC, ^{13}C−^{13}C COSY, ^{1}H−^{15}N-HSQC, ^{1}H−^{15}N-HMBC) were measured in DMSO-d_6 at 25 °C using a Bruker Avance II 300 MHz spectrometer. The ^{13}C NMR spectrum of compound **1** was acquired on an Agilent (Varian) VNMRS 500 MHz spectrometer. LC-MS analyses were performed with a Dionex UltiMate 3000 (Thermo Scientific) coupled with an LCQ Fleet mass spectrometer equipped with an electrospray interface (ESI) and a tridimensional ion trap. The column was an Atlantis T3 C18 5 μm × 4.6 mm × 50 mm maintained at 40 °C at a flow rate of 0.8 mL min^{-1}. Phases A and B were 0.05% TFA and MeCN, respectively. The gradient was 10%, 10%, 95%, 95%, and 10% phase B at 0, 1, 7, 9, and 10 min, respectively. UV−vis signals (190−600 nm) were acquired using a diode array detector. The m/z range was 110−2000, and the ESI conditions were as follows: spray voltage of 3500 V, capillary temperature of 275 °C, sheath gas flow rate at 35 mL min^{-1}, and auxiliary gas flow rate at 15 mL min^{-1}. HR-MS analyses were performed as a service by the Department of Pharmaceutical Sciences, University of Milan, Italy. HPLC analyses were carried out using a Shimadzu LC-2010AHT equipped with a Merck LiChrosphere100 RP18 LiChroCART column, 5 μm (125 × 4 mm) with detection at 280 nm and oven temperature at 50 °C. Flow rate set at 1 mL min^{-1}. Phases A and B were 0.1% TFA and MeCN, respectively. The

DOI: 10.1021/acs.jnatprod.8b00354
J. Nat. Prod. 2019, 82, 35−44

gradient used was 10%, 45%, 70%, and 90% phase B at 0, 5, 15, and 17 min, respectively.

Actinomycete Strains and Growth Conditions. Strains were maintained as frozen cultures at −80 °C in the NAICONS strain library. They were cultivated on S1 plates[10] at 30 °C. All Erlenmeyer flasks used for liquid cultures had one baffle. For production of enduracyclinones the microbial content of one S1 plate was scraped and inoculated into 50 mL Erlenmeyer flasks containing 10 mL of medium AF (dextrose monohydrate 20 g L^{-1}, yeast extract 2 g L^{-1}, soybean meal 8 g L^{-1}, NaCl 1 g L^{-1}, and $CaCO_3$ g L^{-1}, pH 7.3). The strains were grown at 30 °C on an orbital shaker at 200 rpm. After 72 h, 5 mL of the culture was transferred into 500 mL Erlenmeyer flasks containing 100 mL of fresh AF medium. After a further 72 h cultivation as above, a 5% inoculum was made into 100 mL of medium INA5 (glycerol 30 g L^{-1}, soybean meal 15 g L^{-1}, $CaCO_3$ 5 g L^{-1}, NaCl 2 g L^{-1}, pH 7.2) in 500 mL Erlenmeyer flasks, which were incubated for 168 h under the same conditions described above.

Isotope Labeling. NM medium was ammonium sulfate 1.8 g L^{-1}, KH_2PO_4 0.15 g L^{-1}, $MgSO_4{\cdot}7H_2O$ 0.22 g L^{-1}, TMS 3 mL L^{-1}, vitamin solution 1 mL L^{-1}, and 0.5 M TES pH 7.5 40 mL L^{-1}. [TMS consists of (g L^{-1}) $FeSO_4{\cdot}7H_2O$ 5, $CuSO_4{\cdot}5H_2O$ 0.39, $ZnSO_4{\cdot}7H_2O$ 0.44, $MnCl_2{\cdot}4H_2O$ 0.176, $NaMoO_4{\cdot}2H_2O$ 0.011, $CuCl_2{\cdot}2H_2O$ 0.02; and 50 mL HCl 37%; vitamin solution consists of (g L^{-1}) biotin 0.05, Ca pantothenate 1, nicotinic acid 1, myo-inositol 25, thiamine HCl 1, pyridoxine HCl 1; it was sterilized through a 0.22 μm pore filter and added to the autoclaved medium.] Strain ID40491 from a frozen stock was inoculated (5%) in 50 mL flasks containing 15 mL of NM medium supplemented with 10% glycerol and cultivated 72 h as above. Then, 12 mL of the culture was washed twice with 12 mL of medium NM (by centrifugation and resuspension), and 6 mL of the resuspended mycelium was used to inoculate 100 mL of NM medium supplemented with 1 g L^{-1} Celtone base powder (>98% ^{13}C- and >98% ^{15}N-labeled, Cambridge Isotope Laboratories). The strain was cultured under the conditions described above for 120 h before metabolite extraction. The average enrichment was calculated using LC-MS analysis (Supplementary Figure S1), which showed a maximum m/z signal of 749 $[M + H]^+$ with an increment of 38 amu with respect to the unlabeled compound. A full labeled compound **1** is expected to have an m/z 751 $[M + H]^+$; thus the enrichment was calculated as 95%.

Metabolite Extraction and Purification. For purification of enduracyclinones, a 600 mL culture was centrifuged (10 min at 1800 rcf), and the resulting mycelium and cleared broth were processed separately. The mycelium was resuspended in water (200 mL final volume) and, after adjusting the pH from 7.9 to 9.7 with 0.5 N NaOH and adding 200 mL of EtOH, shaken for 20 min at RT. After centrifugation (5 min at 1800 rcf), the supernatant was recovered and dried under vacuum. For processing the cleared broth, the pH was adjusted from 7.5 to 5 with 1 N HCl, which led to product precipitation. The pellet was recovered by centrifugation (10 min at 3200 rcf) and resuspended in 60 mL of water. After adjusting the pH to 9.5 with 0.5 N NaOH and adding 60 mL of EtOH, residual debris was removed by centrifugation (10 min at 1800 rcf) and the solvent from the resulting supernatant was removed under reduced pressure.

The crude extracts from mycelium and cleared broth were separately purified on a CombiFlash RF (Teledyne ISCO) medium-pressure chromatography system on a 30 g Biotage SNAP Cartridge KP-C18-HS. Flow was 30 mL min^{-1}, phase A was water with 0.1% TFA, and phase B was acetonitrile. The column was previously conditioned at 5% phase B, gradient to 40% phase B in 2 min, and then 60% phase B in 25 min. Fractions with similar purity were pooled and dried under vacuum, yielding 90 mg of a dark red powder containing compounds **1** and des-methyl-**1** in a 9:1 ratio. This powder was used for NMR characterization and for nearly all bioactivity studies. From the same chromatography, an additional 35 mg sample was collected containing compounds **1**, **2**, and des-methyl **1** in a 5:3:2 ratio. A 2 mg amount of the 9:1 ratio powder was further purified using an LC 2010A-HT liquid chromatography instrument (Shimadzu Corporation) equipped with a LiChrosphere C18 5 μm, 4.6 mm × 100 mm column (Merck). Elution was performed at 1 mL min^{-1}, 50 °C with a multistep program set as follows: 10%, 45%, 70%, 90%, 90%, 10%, and 10% phase B at 0, 15, 17, 20, 21, and 29 min, respectively. Phase A was 0.1% TFA (v/v) in H_2O, and phase B was CH_3CN. UV detection was set at 270 and 420 nm. About 450 μg of purified compound **1** (enduracyclinone A) was collected and used for MIC evaluation on *S. aureus* ATCC 6538P.

For purification of the labeled compounds, 20 mL of 0.5 M ammonium acetate (pH 8.8) and 110 mL of EtOH were added to a 200 mL culture, and the suspension was shaken 1 h at RT. After centrifugation (10 min 1800 rcf), the supernatant was recovered, partially concentrated under vacuum to remove EtOH, and acidified to pH 4−4.5 with 1 N HCl. Under these conditions enduracyclinones form a dark red precipitate, which was collected by centrifugation (10 min 1800 rcf) and dried under vacuum, obtaining 5 mg of 95% labeled compounds **1** and des-methyl-**1** in a 9:1 ratio.

*Enduracyclinone A, **1**:* HPLC t_R 9.5 min; LC-MS t_R 5.93 min UV−vis (0.1% TFA/MeCN, 1:1) λ_{max} 234, 283, 334, and 445 nm; ^1H and ^{13}C NMR data, Table 1; ESI(+)MS m/z 711.2 $[M + H]^+$; HRESI(+) MS m/z 711.1942 $[M + H]^+$ (calcd for $C_{36}H_{30}N_4O_{12}$ 711.1938).

*Enduracyclinone B, **2**:* HPLC t_R 12 min; LC-MS t_R 6.02 min UV−vis (0.1% TFA/MeCN, 1:1) λ_{max} 241, 295, and 425 nm; ESI(+)MS m/z 713.2 $[M + H]^+$; HRESI(+) MS m/z 713.2104 $[M + H]^+$ (calcd for $C_{36}H_{32}N_4O_{12}$ 713.2095).

Des-methyl Enduracyclinone A: HPLC t_R 10 min; LC-MS t_R 6.48 min UV−vis (0.1% TFA/MeCN, 1:1) λ_{max} 237, 287, 340, and 470 nm; ESI(+)MS m/z 697.2 $[M + H]^+$; HRESI(+) MS m/z 697.1786 $[M + H]^+$ (calcd for $C_{35}H_{28}N_4O_{12}$697.1776).

Chemical Modifications. Reactions were performed on a sample containing **1** and its des-methyl derivative in a 9:1 ratio (designated **1** for simplicity), unless stated otherwise. **Amidation**: Compound **1** (2 mg) was dissolved in 400 μL of DMF, and 2 μL of *N*,*N*-dimethylpropylamine was added adjusting the pH to 8. After adding 2 mg of PyBOP, the mixture was stirred for 1 h at RT. LC-MS analysis showed the disappearance of compound **1** (t_R 5.90 min) and the formation of the corresponding amide (t_R 4.57 min, m/z 795.2 $[M + H]^+$ and 398 $[M + 2H]^{2+}$ and λ_{max} at 245, 285, and 539 nm), along with the formation of des-methyl-**1** corresponding amide (t_R 4.60 min, m/z 781.1 $[M + H]^+$ and 391 $[M + 2H]^{2+}$ and λ_{max} at 247, 292, and 537 nm). **Methylation**: To a solution of **1** (1 mg) in 100 μL of MeOH, was added 4 μL of 2 M trimethylsylyldiazomethane in diethyl ether, and the solution stirred at RT for 5 h. LC-MS analysis showed the disappearance of **1** and formation of one peak at 6.18 min with m/z 725.2 $[M + H]^+$ and λ_{max} at 235, 284, 336, and 440 nm, and a second peak at 6.28 min with m/z 711.3 $[M + H]^+$ and λ_{max} at 243, 288, and 432 nm, corresponding to the methyl esters of **1** and of des-methyl-**1**, respectively. **Oxidation**: Compounds **1**, **2**, and des-methyl-**1** (2 mg, in a 5:3:2 ratio) were dissolved in 2.5 mL of MeCN/H_2O (1:1), and 175 μL of 30% H_2O_2 was added. After 24 h at RT, LC-MS analysis showed the conversion of compound **2** into **1**. **Quinone cleavage**: Compound **1** (1 mg) was dissolved in 50 μL of MeCN/H_2O (1:1), and 100 μL of 30% H_2O_2 was added. The mixture was heated to 60 °C, and the reaction monitored by LC-MS, which showed the formations of peaks at 5.15, 6.30, and 6.72 min corresponding to m/z $[M + H]^+$ values of 637.0 (**ox-1**, λ_{max} at 234, 313, and 420 nm), 469.1 (**ox-2**,major species; λ_{max} at 246, 300, and 430 nm), 455.1 (des-methyl-**ox-2**, minor species), and 279.2 (**ox-3**, λ_{max} at 300 nm), respectively.

Biological Assays. All tests were performed on a sample containing **1** and its des-methyl derivative in a 9:1 ratio. MIC for *S. aureus* ATCC 6538P was determined also for the purified compound **1**. Antimicrobial activity of extracts was evaluated by agar diffusion, using extracts obtained by centrifuging (10 min 1800 rcf) a 10 mL culture and extracting the resulting mycelium with 4 mL of EtOH for 1 h at RT with shaking. The EtOH extracts (200 μL, corresponding to 0.5 mL of culture) were dried under vacuum and dissolved in 100 μL of 10% DMSO, and 10 μL was then deposited on 30 mL of Mueller-Hinton agar in a 14.5 mm diameter plate inoculated with 10^5 CFU/mL *S. aureus* ATCC 6538P or L3797, scoring the presence of growth inhibition halos after 16 h at 37 °C. Determination of minimal inhibitory concentrations (MIC) was performed as previously

DOI: 10.1021/acs.jnatprod.8b00354
J. Nat. Prod. 2019, 82, 35−44

described.[10] Time-kill experiments were performed following a previously described procedure.[11] The conditions for using *Bacillus subtilis* BAU102 to detect cell wall inhibitors or detergents have been previously described.[13]

Effect on Macromolecular Syntheses. The effect on macromolecular synthesis was tested by monitoring the incorporation of labeled precursors (5-[^{3}H]thymidine for DNA, [^{3}H]uridine for RNA, L-[^{3}H]tryptophan for protein and [^{3}H]glucosamine hydrochloride for cell wall synthesis). *S. aureus* 12ST clinical isolate (P.L. proprietary collection) was grown overnight in 0.2× LB (2 g L^{-1} peptone, 1 g L^{-1} yeast extract, and 2 g L^{-1} NaCl), then diluted 200-fold into the same medium, and grown at 37 °C to an OD_{600} of 0.2−0.25. This medium can support fast growth while allowing efficient incorporation of labeled precursors (P.L., unpublished data). Cultures were split into four subcultures (80 μL) and added to Eppendorf tubes containing either 10 μL of medium (control) or 10 μL of **1** at 10-fold the final concentrations. After 5 min incubation at 37 °C, 10 μL of radioactively labeled precursors (PerkinElmer), previously diluted to 0.1 μCi μL^{-1} (1:10), was added as follows: [6-^{3}H]-thymidine, 0.15 μCi/sample; [5,6-^{3}H]-uridine, 0.15 μCi/sample; L-[5-^{3}H(N)]-tryptophan, 0.25 μCi/sample; D-[6-^{3}H(N)]-glucosamine hydrochloride, 0.4 μCi/sample. Samples were incubated for a further 5 min at 37 °C; incorporation was stopped and macromolecules were precipitated by adding 0.9 mL of ice-cold 5% trichloroacetic acid (TCA) and incubated for at least 30 min on ice before being filtered through glass microfiber filters (GF/C, Whatman). Filters were washed with 5 mL of TCA (5%), dried, and counted in a Tricarb 2100 TR liquid scintillation analyzer (PerkinElmer) using the Ultima Gold scintillation cocktail (PerkinElmer). **1** was dissolved at 10 mg mL^{-1} in 50% DMSO immediately prior to use, and subsequent dilutions were made in 0.2× LB. Maximal DMSO concentrations used in the experiment were 0.5%, which did not affect either bacterial growth or incorporation of labeled markers, as tested in preliminary experiments. As controls for macromolecular synthesis inhibition, we used antibiotics with known mechanisms of action, namely, nalidixc acid (25 μg/mL) for DNA synthesis, rifampicin (2 μg/mL) for RNA synthesis, chloramphenicol (20 μg/mL) for protein synthesis, and vancomycin (1 μg/mL) for cell wall synthesis. In the experimental conditions used, these compounds totally and selectively inhibited their target macromolecular synthesis (data not shown).

DNA Sequences. DNA extraction, sequencing, and analysis of the 16S rRNA gene were performed following published procedures.[38] A draft genome sequence of *Nonomuraea* ID40491 was generated through Illumina technology by Microbial Genomics and Biotechnology Center for Biotechnology (Universität Bielefeld, Germany). Identification of the biosynthetic gene cluster was performed using the antiSMASH v3.0.1 tool at the default conditions.[39]

Accession Codes. The DNA sequences of the 16S rRNA genes and putative enduracyclinone gene cluster have been deposited in GenBank with accession numbers MF359959−MF359965 (Supplementary Table S2) and MG386284, respectively.

■ ASSOCIATED CONTENT

Supporting Information

The Supporting Information is available free of charge on the ACS Publications website at DOI: 10.1021/acs.jnatprod.8b00354.

Experimental Section; characteristics of enduracyclinone-producing strains; reporter gene induction assay; time-kill data; cytotoxicity data; macromolecular syntheses inhibition data; ^{13}C−^{15}N enrichment data; NMR spectra (PDF)

■ AUTHOR INFORMATION

Corresponding Author

*E-mail: pmonciardini@naicons.com. Phone: +39 02 56660231.

ORCID

Paolo Monciardini: 0000-0002-8727-2791

Marianna Iorio: 0000-0001-8669-5875

Author Contributions

‖P. Monciardini and A. Bernasconi contributed equally to this work.

Notes

The authors declare the following competing financial interest(s): P.M., A.B., M.I., C.B., M.S., S.M., and S.D. are employees and/or shareholders of NAICONS and/or KtedoGen.

■ ACKNOWLEDGMENTS

This work received support from the European Commission's Horizon 2020 programme under grant agreement 664588 (NOMORFILM project) and from MiUR-Regione Lombardia. We thank I. Biunno and M. Cattaneo (IRGB-CNR, Milan) for the cytotoxicity test, H.-G. Sahl (University of Bonn) for helpful advice, and R. Fattori (IFOM, Milan) for 1D-^{13}C NMR experiment.

■ REFERENCES

(1) Moloney, M. G. *Trends Pharmacol. Sci.* **2016**, *37*, 689−701.
(2) Brown, E. D.; Wright, G. D. *Nature* **2016**, *529*, 336−343.
(3) Bumann, D. *Curr. Opin. Microbiol.* **2008**, *11*, 387−392.
(4) Demain, A. L. *J. Ind. Microbiol. Biotechnol.* **2014**, *41*, 185−201.
(5) Newman, D. J.; Cragg, G. M. *J. Nat. Prod.* **2012**, *75*, 311−335.
(6) Ling, L. L.; Schneider, T.; Peoples, A. J.; Spoering, A. L.; Engels, I.; Conlon, B. P.; Mueller, A.; Schaberle, T. F.; Hughes, D. E.; Epstein, S.; Jones, M.; Lazarides, L.; Steadman, V. A.; Cohen, D. R.; Felix, C. R.; Fetterman, K. A.; Millet, W. P.; Nitti, A. G.; Zullo, A. M.; Chen, C.; Lewis, K. *Nature* **2015**, *517*, 455−459.
(7) Maffioli, S. I.; Zhang, Y.; Degen, D.; Carzaniga, T.; Del Gatto, G.; Serina, S.; Monciardini, P.; Mazzetti, C.; Guglierame, P.; Candiani, G.; Chiriac, A. I.; Facchetti, G.; Kaltofen, P.; Sahl, H. G.; Dehò, G.; Donadio, S.; Ebright, R. H. *Cell* **2017**, *169*, 1240−1248e1223.
(8) Monciardini, P.; Iorio, M.; Maffioli, S.; Sosio, M.; Donadio, S. *Microb. Biotechnol.* **2014**, *7*, 209−220.
(9) Jabes, D.; Donadio, S. *Methods Mol. Biol.* **2010**, *618*, 31−45.
(10) Simone, M.; Monciardini, P.; Gaspari, E.; Donadio, S.; Maffioli, S. I. *J. Antibiot.* **2013**, *66*, 73−78.
(11) Maffioli, S. I.; Monciardini, P.; Catacchio, B.; Mazzetti, C.; Münch, D.; Brunati, C.; Sahl, H. G.; Donadio, S. *ACS Chem. Biol.* **2015**, *10*, 1034−1042.
(12) Iorio, M.; Sasso, O.; Maffioli, S. I.; Bertorelli, R.; Monciardini, P.; Sosio, M.; Bonezzi, F.; Summa, M.; Brunati, C.; Bordoni, R.; Corti, G.; Tarozzo, G.; Piomelli, D.; Reggiani, A.; Donadio, S. *ACS Chem. Biol.* **2014**, *9*, 398−404.
(13) De Pascale, G.; Grigoriadou, C.; Losi, D.; Ciciliato, I.; Sosio, M.; Donadio, S. *J. Appl. Microbiol.* **2007**, *103*, 133−140.
(14) Gerber, N. N.; Lechevalier, M. P. *Can. J. Chem.* **1984**, *62*, 2818−2821.
(15) Rickards, R. W. *J. Antibiot.* **1989**, *42*, 336−339.
(16) Ogawa, H.; Natori, S. *Chem. Pharm. Bull.* **1968**, *16*, 1709−1720.
(17) Cameron, D. W.; Cromartie, R. I. T.; Kingston, D. G. I.; Todd, L. *J. Chem. Soc.* **1964**, *0*, 51−61.
(18) He, H.; Yang, H. Y.; Luckman, S. W.; Bernan, V. S.; Tsai, G.; Roll, D. M.; Carter, G. T. *Helv. Chim. Acta* **2004**, *87*, 1385−1391.
(19) Banskota, A. H.; Aouidate, M.; Sørensen, D.; Ibrahim, A.; Piraee, M.; Zazopoulos, E.; Alarco, A. M.; Gourdeau, H.; Mellon, C.; Farnet, C. M.; Falardeau, P.; McAlpine, J. B. *J. Antibiot.* **2009**, *62*, 565−570.
(20) Winter, D. K.; Sloman, D. L.; Porco, J. A. *Nat. Prod. Rep.* **2013**, *30*, 382−391.

DOI: 10.1021/acs.jnatprod.8b00354
J. Nat. Prod. 2019, 82, 35−44

(21) Aoyama, T.; Kojima, F.; Abe, F.; Muraoka, Y.; Naganawa, H.; Takeuchi, T.; Aoyagi, T. *J. Antibiot.* **1993**, *46*, 914−920.
(22) Atkinson, D. J.; Naysmith, B. J.; Furkert, D. P.; Brimble, M. A. *Beilstein J. Org. Chem.* **2016**, *12*, 2325−2342.
(23) Yin, X.; Zabriskie, T. M. *Microbiology* **2006**, *152*, 2969−2983.
(24) Han, L.; Schwabacher, A. W.; Moran, G. R.; Silvaggi, N. R. *Biochemistry* **2015**, *54*, 7029−7040.
(25) Magarvey, N. A.; Haltli, B.; He, M.; Greenstein, M.; Hucul, J. A. *Antimicrob. Agents Chemother.* **2006**, *50*, 2167−2177.
(26) Zhan, J.; Qiao, K.; Tang, Y. *ChemBioChem* **2009**, *10*, 1447−1452.
(27) Iorio, M.; Cruz, J.; Simone, M.; Bernasconi, A.; Brunati, C.; Sosio, M.; Donadio, S.; Maffioli, S. I. *J. Nat. Prod.* **2017**, *80*, 819−827.
(28) Drautz, H.; Keller-Schierlein, W.; Zähner, H. *Arch. Microbiol.* **1975**, *106*, 175−190.
(29) Nakagawa, A.; Iwai, Y.; Shimizu, H.; Omura, S. *J. Antibiot.* **1986**, *39*, 1636−1638.
(30) Kobayashi, K.; Nishino, C.; Ohya, J.; Sato, S.; Mikawa, T.; Shiobara, Y.; Kodama, M. *J. Antibiot.* **1988**, *41*, 741−750.
(31) Koizumi, Y.; Tomoda, H.; Kumagai, A.; Zhou, X. P.; Koyota, S.; Sugiyama, T. *Cancer Sci.* **2009**, *100*, 322−326.
(32) Zhang, W.; Wang, L.; Kong, L.; Wang, T.; Chu, Y.; Deng, Z.; You, D. *Chem. Biol.* **2012**, *19*, 422−432.
(33) Tanaka, H.; Kawakita, K.; Suzuki, H.; Spiri-Nakagawa, P.; Omura, S. *J. Antibiot.* **1989**, *42*, 431−439.
(34) Liu, L. L.; He, L. S.; Xu, Y.; Han, Z.; Li, Y. X.; Zhong, J. L.; Guo, X. R.; Zhang, X. X.; Ko, K. M.; Qian, P. Y. *Chem. Res. Toxicol.* **2013**, *26*, 1055−1063.
(35) Suzukake, K.; Hori, M. *J. Antibiot.* **1977**, *30*, 132−140.
(36) Müller, A.; Klöckner, A.; Schneider, T. *Nat. Prod. Rep.* **2017**, *34*, 909−932.
(37) Medema, M. H.; Kottmann, R.; Yilmaz, P.; Cummings, M.; Biggins, J. B.; Blin, K.; de Bruijn, I.; Chooi, Y. H.; Claesen, J.; Coates, R. C.; Cruz-Morales, P.; Duddela, S.; Düsterhus, S.; Edwards, D. J.; Fewer, D. P.; Garg, N.; Geiger, C.; Gomez-Escribano, J. P.; Greule, A.; Hadjithomas, M.; Haines, A. S.; Helfrich, E. J.; Hillwig, M. L.; Ishida, K.; Jones, A. C.; Jones, C. S.; Jungmann, K.; Kegler, C.; Kim, H. U.; Kötter, P.; Krug, D.; Masschelein, J.; Melnik, A. V.; Mantovani, S. M.; Monroe, E. A.; Moore, M.; Moss, N.; Nützmann, H. W.; Pan, G.; Pati, A.; Petras, D.; Reen, F. J.; Rosconi, F.; Rui, Z.; Tian, Z.; Tobias, N. J.; Tsunematsu, Y.; Wiemann, P.; Wyckoff, E.; Yan, X.; Yim, G.; Yu, F.; Xie, Y.; Aigle, B.; Apel, A. K.; Balibar, C. J.; Balskus, E. P.; Barona-Gómez, F.; Bechthold, A.; Bode, H. B.; Borriss, R.; Brady, S. F.; Brakhage, A. A.; Caffrey, P.; Cheng, Y. Q.; Clardy, J.; Cox, R. J.; De Mot, R.; Donadio, S.; Donia, M. S.; van der Donk, W. A.; Dorrestein, P. C.; Doyle, S.; Driessen, A. J.; Ehling-Schulz, M.; Entian, K. D.; Fischbach, M. A.; Gerwick, L.; Gerwick, W. H.; Gross, H.; Gust, B.; Hertweck, C.; Höfte, M.; Jensen, S. E.; Ju, J.; Katz, L.; Kaysser, L.; Klassen, J. L.; Keller, N. P.; Kormanec, J.; Kuipers, O. P.; Kuzuyama, T.; Kyrpides, N. C.; Kwon, H. J.; Lautru, S.; Lavigne, R.; Lee, C. Y.; Linquan, B.; Liu, X.; Liu, W.; Luzhetskyy, A.; Mahmud, T.; Mast, Y.; Méndez, C.; Metsä-Ketelä, M.; Micklefield, J.; Mitchell, D. A.; Moore, B. S.; Moreira, L. M.; Müller, R.; Neilan, B. A.; Nett, M.; Nielsen, J.; O'Gara, F.; Oikawa, H.; Osbourn, A.; Osburne, M. S.; Ostash, B.; Payne, S. M.; Pernodet, J. L.; Petricek, M.; Piel, J.; Ploux, O.; Raaijmakers, J. M.; Salas, J. A.; Schmitt, E. K.; Scott, B.; Seipke, R. F.; Shen, B.; Sherman, D. H.; Sivonen, K.; Smanski, M. J.; Sosio, M.; Stegmann, E.; Süssmuth, R. D.; Tahlan, K.; Thomas, C. M.; Tang, Y.; Truman, A. W.; Viaud, M.; Walton, J. D.; Walsh, C. T.; Weber, T.; van Wezel, G. P.; Wilkinson, B.; Willey, J. M.; Wohlleben, W.; Wright, G. D.; Ziemert, N.; Zhang, C.; Zotchev, S. B.; Breitling, R.; Takano, E.; Glöckner, F. O. *Nat. Chem. Biol.* **2015**, *11*, 625−631.
(38) Mazza, P.; Monciardini, P.; Cavaletti, L.; Sosio, M.; Donadio, S. *Microb. Ecol.* **2003**, *45*, 362−72.
(39) Weber, T.; Blin, K.; Duddela, S.; Krug, D.; Kim, H. U.; Bruccoleri, R.; Lee, S. Y.; Fischbach, M. A.; Müller, R.; Wohlleben, W.; Breitling, R.; Takano, E.; Medema, M. H. *Nucleic Acids Res.* **2015**, *43*, W237−43.

DOI: 10.1021/acs.jnatprod.8b00354
J. Nat. Prod. 2019, 82, 35−44